ASTRONOMY

ASASSN-15lh: A highly super-luminous supernova

Subo Dong,[1*] B. J. Shappee,[2] J. L. Prieto,[3,4] S. W. Jha,[5] K. Z. Stanek,[6,7] T. W.-S. Holoien,[6,7] C. S. Kochanek,[6,7] T. A. Thompson,[6,7] N. Morrell,[8] I. B. Thompson,[2] U. Basu,[6] J. F. Beacom,[6,7,9] D. Bersier,[10] J. Brimacombe,[11] J. S. Brown,[6] F. Bufano,[12] Ping Chen,[13] E. Conseil,[14] A. B. Danilet,[6] E. Falco,[15] D. Grupe,[16] S. Kiyota,[17] G. Masi,[18] B. Nicholls,[19] F. Olivares E.,[4,20] G. Pignata,[4,20] G. Pojmanski,[21] G. V. Simonian,[6] D. M. Szczygiel,[21] P. R. Woźniak[22]

We report the discovery of ASASSN-15lh (SN 2015L), which we interpret as the most luminous supernova yet found. At redshift z = 0.2326, ASASSN-15lh reached an absolute magnitude of $M_{u,\mathrm{AB}} = -23.5 \pm 0.1$ and bolometric luminosity $L_{\mathrm{bol}} = (2.2 \pm 0.2) \times 10^{45}$ ergs s^{-1}, which is more than twice as luminous as any previously known supernova. It has several major features characteristic of the hydrogen-poor super-luminous supernovae (SLSNe-I), whose energy sources and progenitors are currently poorly understood. In contrast to most previously known SLSNe-I that reside in star-forming dwarf galaxies, ASASSN-15lh appears to be hosted by a luminous galaxy ($M_K \approx -25.5$) with little star formation. In the 4 months since first detection, ASASSN-15lh radiated $(1.1 \pm 0.2) \times 10^{52}$ ergs, challenging the magnetar model for its engine.

Only within the past two decades has the most luminous class of supernovae (super-luminous supernovae, SLSNe) been identified (*1*). Compared with the most commonly discovered SNe (Type Ia), SLSNe are more luminous by over two magnitudes at peak and rarer by at least 3 orders of magnitude (*2*). Like normal SNe, SLSNe are classified by their spectra as either SLSN-I (hydrogen-poor) or SLSN-II (hydrogen-rich). Yet, the physical characteristics of SLSNe may not be simple extensions from their low-luminosity counterparts (*1*). In particular, the power source for SLSNe-I is poorly understood (*3*). Adding to the puzzle, SLSNe tend to explode in low-luminosity, star-forming dwarf galaxies (*4*–*6*). The recent advent of wide-area, untargeted transient surveys has made the systematic discovery and investigation of the SLSNe population possible [(*7*, *8*) and references therein].

The All-Sky Automated Survey for SuperNovae [ASAS-SN; www.astronomy.ohio-state.edu/~assassin (*9*)] scans the visible sky every two to three nights to depths of $V \approx 16.5$ to 17.3 mag using a global network of 14-cm telescopes (*9*) in an untargeted search for new transients, particularly bright supernovae.

On 14 June 2015 (universal time dates are used throughout this paper), ASAS-SN triggered on a new source located at RA = 22^{h}02^{m}15^{s}.45 Dec = −61°39′34″.6 (J2000), coinciding with a galaxy of then unknown redshift, APMUKS(BJ) B215839.70−615403.9 (*10*). Upon confirmation with our follow-up telescopes, we designated this new source ASASSN-15lh and published its coordinates (*11*).

By combining multiple epochs of ASAS-SN images, we extended the detections to fainter fluxes, finding prediscovery images of ASASSN-15lh from 8 May 2015 (V = 17.39 ± 0.23 mag), and the light curve through 19 September 2015 is shown in Fig. 1. The ASAS-SN light curve peaked at V = 16.9 ± 0.1 on approximately t_{peak} ~ JD2457179 (2015 June 05) based on a parabolic fit to the lightcurve (Fig. 1, dashed line). Follow-up images were taken with the Las Cumbres Observatory Global Telescope Network (LCOGT) 1-m telescopes, and the *BV* light-curves with the galaxy contribution subtracted are also shown.

We obtained an optical spectrum (3700 to 9200 Å) of ASASSN-15lh on 21 June 2015 with the du Pont 100-inch telescope. The steep spectral slope with relatively high blue flux motivated *Swift* UltraViolet and Optical Telescope (UVOT)/X-Ray Telescope (XRT) (*12*) target-of-opportunity observations starting on 24 June 2015. The six-band *Swift* light curve spanning from the ultraviolet (UV) to the optical (1928 to 5468 Å) is shown in Fig. 1. The *Swift* spectral energy distribution (SED), peaking in the UV, indicates that the source has a high temperature. We derive a 3σ x-ray flux limit of $<1.6 \times 10^{-14}$ ergs s^{-1} cm^{-2} (0.3 to 10 keV) from a total XRT exposure of 81 ks taken between 24 June and 18 September 2015.

The du Pont spectrum is mostly featureless (Fig. 2A, first from the top), except for a deep, broad absorption trough near ~5100 Å (observer frame). SNID (*13*), a commonly used SN classification software that has a spectral library of most types of supernovae except SLSN, failed to find a good SN match. However, we noticed a resemblance between the trough and a feature attributed to O II absorption near 4100 Å (rest frame) in the spectrum of PTF10cwr/SN 2010gx, a SLSN-I at z = 0.230 (*3*, *14*, *15*). Assuming that the ASASSN-15lh absorption trough (full width at half maximum of ~10^{4} km s^{-1}) was also due to the same feature indicated a similar redshift of z ~ 0.23. An optical spectrum (3250 to 6150 Å) obtained on the Southern African Large Telescope (SALT) revealed a clear Mg II absorption doublet (λλ2796, 2803) at z = 0.232, confirming the redshift expected from our tentative line identification. Subsequent Magellan/Clay (6 July) and SALT (7 July) spectra refined the redshift to z = 0.2326 (Fig. 2, C and D). The available rest frame spectra show continua with steep spectral slope, relatively high blue fluxes, and several broad absorption features also seen in PTF10cwr/SN 2010gx (Fig. 2A, features "a," "b," and "c") and without hydrogen or helium features, which is consistent with the main spectral features of SLSNe-I (*1*, *3*). The broad absorption feature near 4400 Å (Fig. 2, "d") seen in PTF10cwr/SN 2010gx is not present in ASASSN-15lh. ASASSN-15lh thus has some distinct spectral characteristics in comparison with PTF10cwr/SN 2010gx and some other SLSNe-I (*3*).

Using a luminosity distance of 1171 Mpc (standard *Planck* cosmology at z = 0.2326), Galactic extinction of $E(B-V)$ = 0.03 mag (*16*), assuming no host extinction (thus, the luminosity derived is likely a lower limit), and fitting the *Swift* and LCOGT flux measurements to a simple blackbody (BB) model, we obtain declining rest-frame temperatures of T_{BB} from 2.1×10^{4} to 1.3×10^{4} K and bolometric luminosities of $L_{\mathrm{bol}} = 2.2 \times 10^{45}$ to 0.4×10^{45} ergs s^{-1} at rest-frame phases relative to the peak of t_{rest} ~ 15 and ~50 days, respectively (Fig. 3). ASASSN-15lh's bolometric magnitude declines at a best-fit linear rate of 0.048 mag day^{-1}, which is practically identical to SLSN-I iPTF13ajg (*17*) at 0.049 mag day^{-1} during similar phases (~10 to ~50 days). Subsequently, the luminosity and temperature reach a "plateau" phase with slow changes, and a similar trend is also seen for iPTF13ajg though with sparser coverage. Overall,

[1]Kavli Institute for Astronomy and Astrophysics, Peking University, Yi He Yuan Road 5, Hai Dian District, Beijing 100871, China. [2]Carnegie Observatories, 813 Santa Barbara Street, Pasadena, CA 91101, USA. [3]Núcleo de Astronomía de la Facultad de Ingeniería, Universidad Diego Portales, Av. Ejército 441, Santiago, Chile. [4]Millennium Institute of Astrophysics, Santiago, Chile. [5]Department of Physics and Astronomy, Rutgers, The State University of New Jersey, 136 Frelinghuysen Road, Piscataway, NJ 08854, USA. [6]Department of Astronomy, The Ohio State University, 140 W. 18th Avenue, Columbus, OH 43210, USA. [7]Center for Cosmology and AstroParticle Physics (CCAPP), The Ohio State University, 191 W. Woodruff Avenue, Columbus, OH 43210, USA. [8]Las Campanas Observatory, Carnegie Observatories, Casilla 601, La Serena, Chile. [9]Department of Physics, The Ohio State University, 191 W. Woodruff Avenue, Columbus, OH 43210, USA. [10]Astrophysics Research Institute, Liverpool John Moores University, 146 Brownlow Hill, Liverpool L3 5RF, UK. [11]Coral Towers Observatory, Cairns, Queensland 4870, Australia. [12]INAF-Osservatorio Astrofisico di Catania, Via S.Sofia 78, 95123, Catania, Italy. [13]Department of Astronomy, Peking University, Yi He Yuan Road 5, Hai Dian District, 100871, P. R. China. [14]Association Francaise des Observateurs d'Etoiles Variables (AFOEV), Observatoire de Strasbourg 11, rue de l'Université, F-67000 Strasbourg, France. [15]Harvard-Smithsonian Center for Astrophysics, 60 Garden Street, Cambridge, MA 02138, USA. [16]Department of Earth and Space Science, Morehead State University, 235 Martindale Drive, Morehead, KY 40351, USA. [17]Variable Star Observers League in Japan (VSOLJ), 7-1 Kitahatsutomi, Kamagaya, Chiba 273-0126, Japan. [18]The Virtual Telescope Project, Via Madonna de Loco 47, 03023 Ceccano, Italy. [19]Mt Vernon Observatory, 6 Mt Vernon pl, Nelson, New Zealand. [20]Departamento Ciencias Fisicas, Universidad Andres Bello, Av. Republica 252, Santiago, Chile. [21]Warsaw University Astronomical Observatory, Al. Ujazdowskie 4, 00-478 Warsaw, Poland. [22]Los Alamos National Laboratory, Mail Stop B244, Los Alamos, NM 87545, USA.
***Corresponding author. E-mail: dongsubo@pku.edu.cn**

the temperature and luminosity time evolution resemble iPTF13ajg, but ASASSN-15lh has a systematically higher temperature at similar phases. The estimated BB radius of ~5×10^{15} cm near the peak is similar to those derived for other SLSNe-I (*3*, *17*). These similarities in the evolution of key properties support the argument that ASASSN-15lh is a member of the SLSN-I class, but with extreme properties.

The absolute magnitudes (AB) in the rest-frame u-band are shown in Fig. 4. Using either T_{BB} or the spectra, there is little K-correction (*18*) in converting from B-band to rest-frame u_{AB} with $K_{B\rightarrow u_{AB}} = -0.1$. The solid red points at $t_{rest} \gtrsim$ 10 days include B-band data. Before ~10 days, we lack measurements in blue bands. To estimate $M_{u,AB}$ at these earlier epochs, we assumed the $B - V = -0.3$ mag color and K-corrections found for the later epochs with *Swift* photometry. We estimate an integrated bolometric luminosity radiated of ~$(1.1 \pm 0.2) \times 10^{52}$ ergs over 108 days in the rest frame. Although our estimates at $t_{rest} \lesssim 10$ days should be treated with caution, we can securely conclude that the peak $M_{u,AB}$ is at or brighter than -23.5 ± 0.1, with a bolometric luminosity at or greater than $(2.2 \pm 0.2) \times 10^{45}$ ergs s^{-1}. Both values are without precedent for any supernova recorded in the literature. In Fig. 4, we compare ASASSN-15lh with a sample of SLSNe-I (*3*, *17*). Although its spectra resemble the SLSNe-I subclass, ASASSN-15lh stands out from the luminosity distribution of known SLSNe-I, whose luminosities are narrowly distributed around $M \sim -21.7$ (*2*, *19*). In table S1, we list the peak luminosities of the five most luminous SNe discovered to date, including both SLSN-I and SLSN-II. The spectral correspondence and similarities in temperature, luminosity, and radius evolutions between ASASSN-15lh and some SLSNe-I lead to the conclusion that ASASSN-15lh is the most luminous supernova yet discovered. Even though we find that SLSN-I is the most plausible classification of ASASSN-15lh, it is important to consider other interpretations given its distinct properties. We discuss alternative physical interpretations of ASASSN-15lh in the supplementary text, and given all the currently available data, we conclude that it is most likely a supernova, albeit an extreme one.

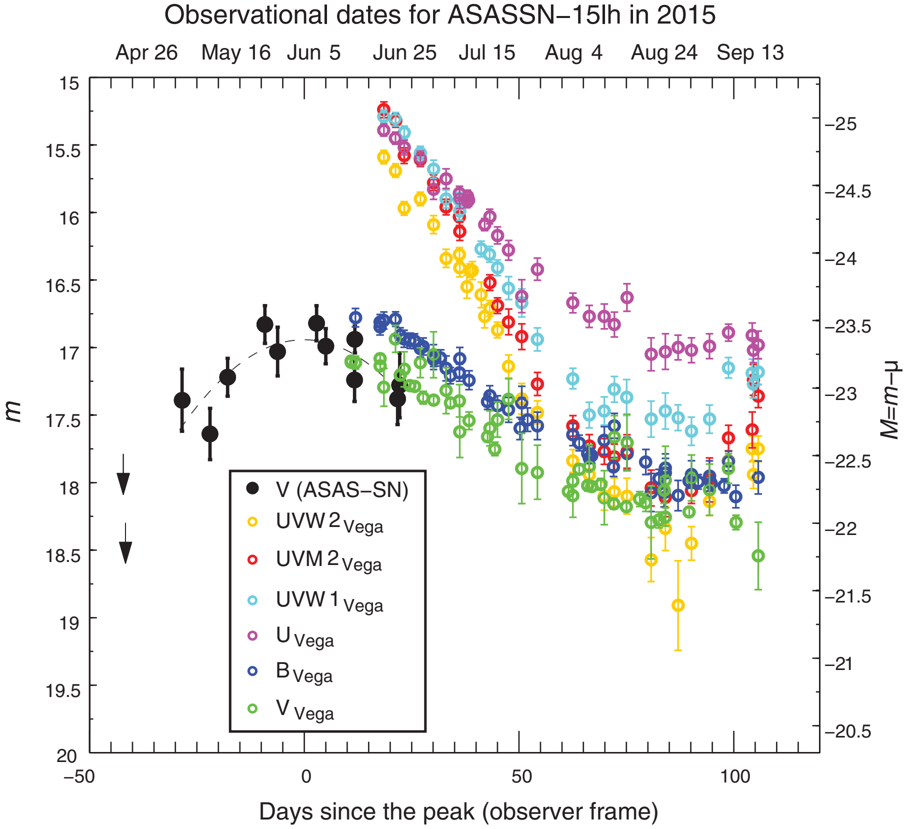

Fig. 1. Multi-band light curve of ASASSN-15lh. The V-band ASAS-SN light curve is shown as black solid dots, and upper limits are represented by black arrows. *Swift* and LCOGT 1-m data are shown as open circles.

Fig. 2. Rest-frame spectra of ASASSN-15lh (black) compared with SLSN-I PTF10cwr/SN 2010gx (red). (**A**) The spectra are offset for clarity, labeled with phases and telescopes, and ranked by descending T_{BB} (given on the right) from the top. The ASASSN-15lh spectra are blue and featureless, except for broad absorption features labeled "a," "b," and "c" (marked in blue), which match those of PTF10cwr/SN 2010gx at similar T_{BB}. Absorption features "a" at ~4100 Å and "d" at ~4400 Å (marked in red) in PTF10cwr/SN 2010gx are commonly attributed to O II (*3*, *15*). The ~4400 Å feature is not present in ASASSN-15lh. (**B**) Close-ups of the 4100 Å features, whose evolution in shape, depth, and velocity as a function of T_{BB} is similar for both supernovae. (**C** and **D**) The ASASSN-15lh host redshift (z = 0.2326) is determined from the Mg II doublets seen in the SALT and Clay MagE spectra, with EW 0.55 ± 0.05 and 0.49 ± 0.05 Å in (C) and (D), respectively.

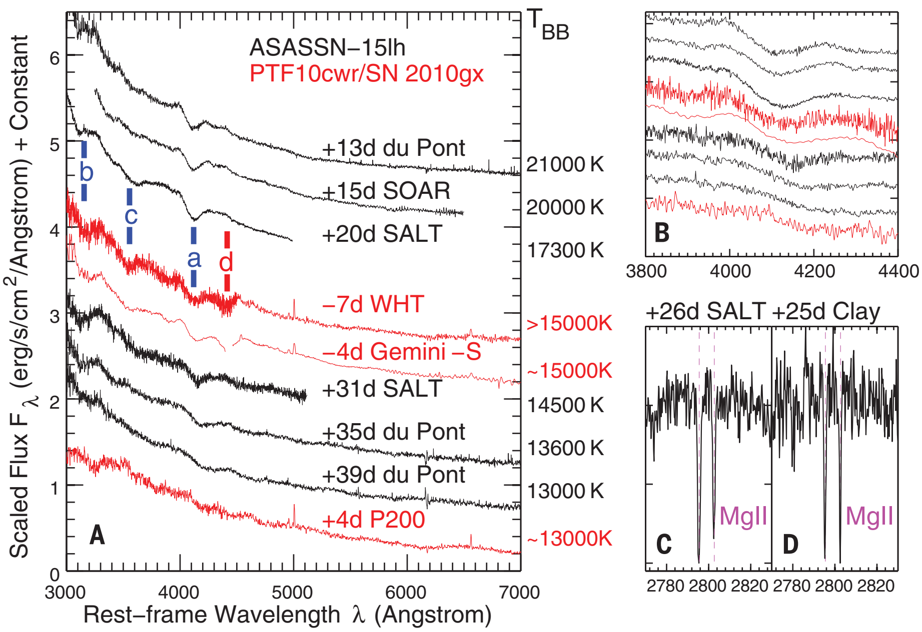

The rate of events with similar luminosities to ASASSN-15lh is uncertain. On the basis of a simple model of transient light curves in ASAS-SN observations tuned to reproduce the magnitude distribution of ASAS-SN Type Ia supernovae (supplementary text), the discovery of one ASASSN-15lh–like event implies a rate of $r \simeq 0.6\ \mathrm{Gpc}^{-3}\ \mathrm{yr}^{-1}$ (90% confidence: $0.21 < r < 2.8$). This is at least 2 times and can be as much as 100 times smaller than the overall rate of SLSNe-I, $r \simeq 32\ \mathrm{Gpc}^{-3}\ \mathrm{yr}^{-1}$ (90% confidence: $6 < r < 109$) from (*2*), and suggests a steeply falling luminosity function for such supernovae.

For a redshift of $z = 0.2326$, the host galaxy of ASASSN-15lh has $M_K \approx -25.5$, which is much more luminous than the Milky Way. We estimate an effective radius for the galaxy of 2.4 ± 0.3 kpc and a stellar mass of $M_* \approx 2 \times 10^{11}\ M_\odot$. This is in contrast to the host galaxies of other SLSNe, which tend to have much lower M_* (*4*–*6*). However, given the currently available data, we cannot rule out the possibility that the host is a dwarf satellite galaxy seen in projection. The lack of narrow hydrogen and oxygen emission lines from the galaxy superimposed in the supernova spectra implies little star formation (SFR) $< 0.3\ M_\odot\ \mathrm{yr}^{-1}$ by applying the conversions in (*20*). Las Cumbres Observatory Global Telescope (LCOGT) astrometry places ASASSN-15lh within 0″.2 (750 pc) of the center of the nominal host. A detailed discussion of the host properties is provided in the supplementary text.

The power source for ASASSN-15lh is unknown. Traditional mechanisms invoked for normal SNe likely cannot explain SLSNe-I (*3*). The lack of hydrogen or helium suggests that shock interactions with hydrogen-rich circumstellar material, invoked to interpret some SLSNe, cannot explain SLSNe-I or ASASSN-15lh. SLSN-I post-peak decline rates appear too fast to be explained by the radioactive decay of ^{56}Ni (*3*)—the energy source for Type Ia supernovae. Both the decline rate of the late-time light curve and the integral method (*21*) will allow tests of whether ASASSN-15lh is powered by ^{56}Ni, and we estimate that $\gtrsim 30\ M_\odot$ of ^{56}Ni would be required to produce ASASSN-15lh's peak luminosity. Another possibility is that the spindown of a rapidly rotating, highly magnetic neutron star (a magnetar) powers the extraordinary emission (*22*–*24*). To match the peak L_{bol} and time scale of ASASSN-15lh, the light-curve models of (*23*) imply a magnetar spin period and magnetic field strength of $P \simeq 1$ ms and $B \simeq 10^{14}$ G, respectively, assuming that all of the spindown power is thermalized in the stellar envelope. If efficient thermalization continues, this model predicts a $L_{\mathrm{bol}} \propto t^{-2}$ power-law at late times. The total observed energy radiated so far ($1.1 \pm 0.2 \times 10^{52}$ ergs) strains a magnetar interpretation because, for $P \lesssim 1$ ms, gravitational wave radiation should limit the total rotational energy available to $E_{\mathrm{rot}}^{\mathrm{max}} \sim 3 \times 10^{52}$ ergs (*25*) and the total radiated energy to a third of $E_{\mathrm{rot}}^{\mathrm{max}}$, which is $\sim 10^{52}$ ergs (*23*).

The extreme luminosity of ASASSN-15lh opens up the possibility of observing such supernovae in the early universe. An event similar to ASASSN-15lh could be observed with the Hubble Space Telescope out to $z \sim 6$, and with the James Webb Space Telescope out to $z \gtrsim 10$ (*19*). A well-observed local counterpart will be critical in making sense of future observations of the transient high-redshift universe.

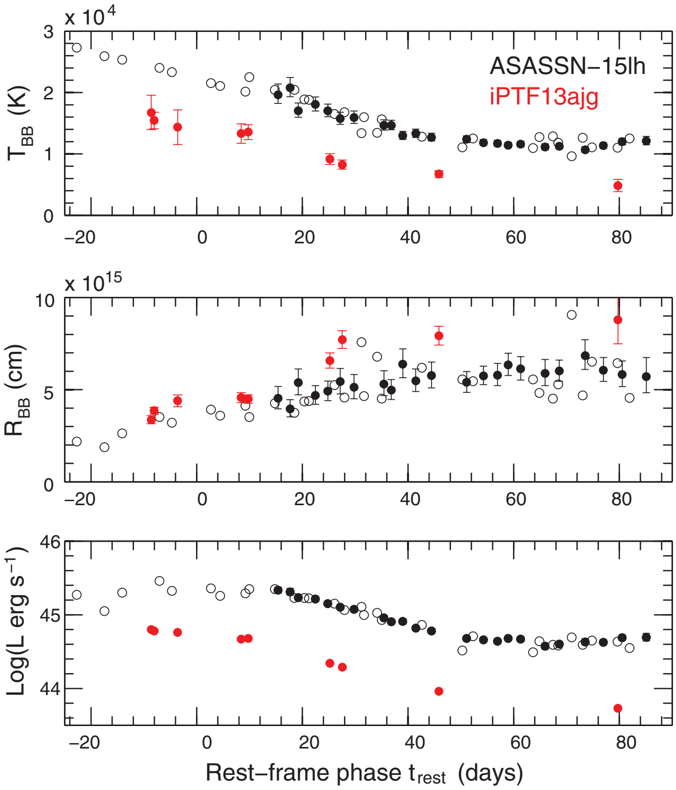

Fig. 3. Time evolution of blackbody temperatures, radii and bolometric luminosities for ASASSN-15lh (black) and SLSN-I iPTF13ajg (red). Solid black dots show estimates derived from the full UV and optical bands, whereas the open circles show those from optical only. For $t_{\mathrm{rest}} < 10$ days, only *V*-band is available, and the temperatures are estimated on the basis of linear extrapolation from MJD = 57191 – 57241.

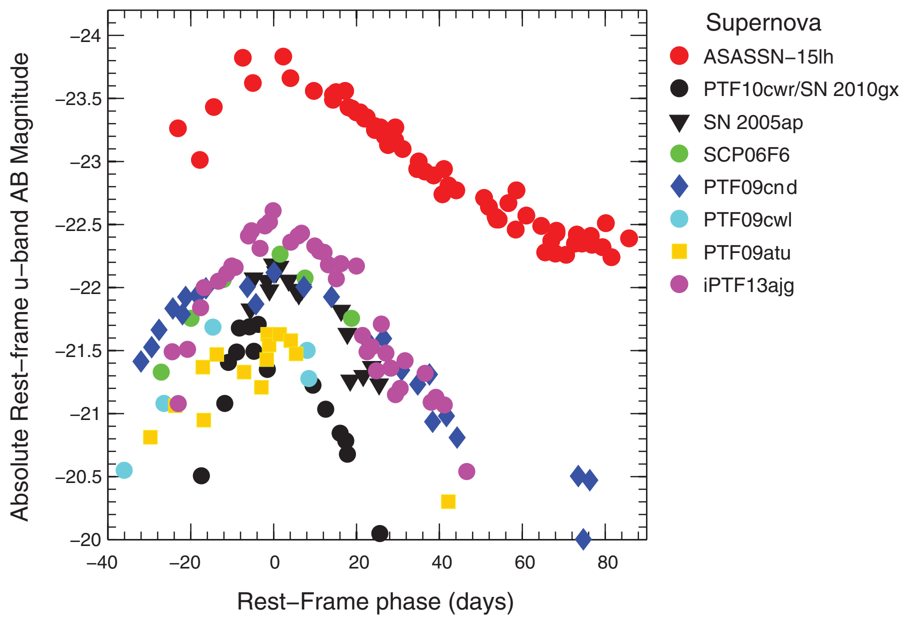

Fig. 4. Rest-frame absolute magnitude light curve of ASASSN-15lh near peak compared with other SLSNe-I. Estimates of $M_{u,\mathrm{AB}}$ for ASASSN-15lh at $t_{\mathrm{rest}} \gtrsim 10$ days are derived from *B*-band fluxes, which are subject to small K-corrections, whereas the less reliable $M_{u,\mathrm{AB}}$ estimates are based on *V*-band only for $t_{\mathrm{rest}} \lesssim 10$ days. The comparison sample (*3*, *17*) includes the most luminous SLSNe-I previously known. At $M_{u,\mathrm{AB}} = -23.5$, ASASSN-15lh stands out from the SLSNe-I luminosity distribution (*2*, *19*). Its peak bolometric absolute magnitude is more than ~1 mag more luminous than any other SLSN-I.

REFERENCES AND NOTES

1. A. Gal-Yam, *Science* **337**, 927–932 (2012).
2. R. M. Quimby, F. Yuan, C. Akerlof, J. C. Wheeler, *Mon. Not. R. Astron. Soc.* **431**, 912–922 (2013).
3. R. M. Quimby *et al.*, *Nature* **474**, 487–489 (2011).
4. J. D. Neill *et al.*, *Astrophys. J.* **727**, 15 (2011).
5. R. Stoll *et al.*, *Astrophys. J.* **730**, 34 (2011).
6. R. Lunnan *et al.*, *Astrophys. J.* **787**, 138 (2014).
7. R. M. Quimby, in *IAU Symposium*, A. Ray, R. A. McCray, Eds. (International Astronomical Union, 2014), vol. 296, pp. 68–76.
8. M. Nicholl *et al.*, *Mon. Not. R. Astron. Soc.* **452**, 3869–3893 (2015).
9. B. J. Shappee *et al.*, *Astrophys. J.* **788**, 48 (2014).
10. S. J. Maddox, G. Efstathiou, W. J. Sutherland, J. Loveday, *Mon. Not. R. Astron. Soc.* **243**, 692 (1990).
11. B. Nicholls *et al.*, *Astronomer's Telegram* **7642**, 1 (2015).
12. D. N. Burrows *et al.*, *Space Sci. Rev.* **120**, 165–195 (2005).
13. S. Blondin, J. L. Tonry, *Astrophys. J.* **666**, 1024–1047 (2007).
14. A. Pastorello *et al.*, *Astrophys. J.* **724**, L16–L21 (2010).
15. C. Inserra *et al.*, *Astrophys. J.* **770**, 128 (2013).
16. E. F. Schlafly, D. P. Finkbeiner, *Astrophys. J.* **737**, 103 (2011).
17. P. M. Vreeswijk *et al.*, *Astrophys. J.* **797**, 24 (2014).
18. D. W. Hogg, I. K. Baldry, M. R. Blanton, D. J. Eisenstein, *ArXiv Astrophysics e-prints:astro-ph/0210394* (2012).
19. C. Inserra, S. J. Smartt, *Astrophys. J.* **796**, 87 (2014).
20. S. Savaglio, K. Glazebrook, D. Le Borgne, *Astrophys. J.* **691**, 182–211 (2009).
21. B. Katz, D. Kushnir, S. Dong, http://arxiv.org/abs/1301.6766 (2013).
22. P. Bodenheimer, J. P. Ostriker, *Astrophys. J.* **191**, 465 (1974).
23. D. Kasen, L. Bildsten, *Astrophys. J.* **717**, 245–249 (2010).
24. S. E. Woosley, *Astrophys. J.* **719**, L204–L207 (2010).
25. B. D. Metzger, D. Giannios, T. A. Thompson, N. Bucciantini, E. Quataert, *Mon. Not. R. Astron. Soc.* **413**, 2031–2056 (2011).
26. O. Yaron, A. Gal-Yam, *Publ. Astron. Soc. Pac.* **124**, 668–681 (2012).

ACKNOWLEDGMENTS

We acknowledge B. Zhang, L. Ho, A. Gal-Yam, and B. Katz for comments; NSF AST-1515927, OSU CCAPP, Mt. Cuba Astronomical Foundation, TAP, SAO, CAS grant XDB09000000 (S.D.); NASA Hubble Fellowship (B.J.S.); FONDECYT grant 1151445, MAS project IC120009 (J.L.P.); NSF CAREER award AST-0847157 (S.W.J.); U.S. Department of Energy (DOE) DE-FG02-97ER25308 (T.W.-S.H.); NSF PHY-1404311 (J.F.B.); D. Victor for donating equipment (BN); FONDECYT postdoctoral fellowship 3140326 (F.O.E.), and Los Alamos National Laboratory Laboratory Directed Research and Development program (P.R.W). B.J.S. is a Hubble and Carnegie-Princeton Fellow. All data used in this paper are made public, including the photometric data (tables S1 to S6) and spectroscopic data at public repository WISeREP (*26*) (http://wiserep.weizmann.ac.il).

SUPPLEMENTARY MATERIALS

www.sciencemag.org/content/351/6270/257/suppl/DC1
Materials and Methods
Supplementary Text
Figures S1 to S5
Tables S1 to S6
References (*27*–*65*)

10 July 2015; accepted 24 November 2015
10.1126/science.aac9613

PALEOANTHROPOLOGY

Early human presence in the Arctic: Evidence from 45,000-year-old mammoth remains

Vladimir V. Pitulko,[1]*† Alexei N. Tikhonov,[2]* Elena Y. Pavlova,[3] Pavel A. Nikolskiy,[4] Konstantin E. Kuper,[5] Roman N. Polozov[6]

Archaeological evidence for human dispersal through northern Eurasia before 40,000 years ago is rare. In west Siberia, the northernmost find of that age is located at 57°N. Elsewhere, the earliest presence of humans in the Arctic is commonly thought to be circa 35,000 to 30,000 years before the present. A mammoth kill site in the central Siberian Arctic, dated to 45,000 years before the present, expands the populated area to almost 72°N. The advancement of mammoth hunting probably allowed people to survive and spread widely across northernmost Arctic Siberia.

Evidence for human habitation in the Arctic before the Last Glacial Maximum (LGM), which spans 26.5 to 19 thousand years ago (ka) (*1*), is very rare (Fig. 1A and fig. S1). It has only become available in the past 20 years, with the discoveries of the Mamontovaya Kurya site (*2*) in the European Arctic and the Yana Rhinoceros Horn Site (RHS) in Arctic Siberia (*3*). Before these discoveries, researchers held that humans could not have started populating the Arctic regions until the Pleistocene-Holocene boundary (*4*). The recent discoveries indicate the presence of people in the Arctic at least at the end of marine isotope stage 3 (MIS 3), around 28,000 ^{14}C years before the present (yr B.P.) or slightly earlier, whereas older sites are found south of 55°N.

Archaeological evidence for human dispersal throughout northern Eurasia dated to the first half of MIS 3 is known from different areas (*5*–*10*). In Siberia, this evidence is concentrated far south of the Arctic circle (*7*–*11*). In addition to some dozen sites with age estimates within ~45 to 30 ka, which are well supported by reliable data, there are several controversial localities in northeast Europe (*12*, *13*), the Urals (*14*), and Siberia (*9*, *10*). Thus, the relevant archaeological record for all of northern Eurasia amounts to 15 to 20 contexts with a northern latitudinal limit of 55°N (fig. S1). In west Siberia, a human fossil with an early modern human genome was recently found at 57°N and produced a direct radiocarbon date of 45,000 yr B.P.; however, these remains were not found in an archaeological context (*15*). Thus, the archaeological record for northern Eurasia has not suggested human presence in the Arctic that early, although there is evidence firmly dated to ~30 ka (*3*).

Ice sheet expansion during MIS 4 did not affect most of the Siberian Arctic (*16*). Interglacial (MIS 3) environmental conditions varied across the Eurasian Arctic (*17*–*21*) but were overall beneficial for the growth of late Pleistocene large herbivore populations, including mammoths, in various parts of the region (*22*–*25*). At the end of MIS 3, mammoths moved into deglaciated areas (*26*) and offered an unlimited food source, supporting the pre-LGM human settlement now corroborated for both the European and eastern Siberian Arctic (*2*, *3*, *25*, *26*).

The central Siberian Arctic was also populated by mammoths for a long time (*22*, *27*). Reconstructed fluctuations of their population numbers (*22*) largely follow the pattern seen among the mammoth populations in the New Siberian Islands and Northern Yana-Indighirka lowland. One of the highest peaks of the mammoth population numbers occurred around 44 to 42 ka (*25*).

In 2012, a team led by one of us (Tikhonov) excavated a partial carcass of a woolly mammoth (*Mammuthus primigenius*, Blumenbach, 1799) from frozen sediments exposed in a coastal bluff on the eastern shore of Yenisei Bay, 1.8 km north of the Sopochnaya Karga (SK) meteorological station, at 71°54′19.2″N and 82°4′23.5″E (Fig. 1B). The exposure stratigraphy there is composed of several clear structural elements (*28*).

Several radiocarbon dates help anchor this sequence in time (Fig. 1, C and D, and table S1). The peat layer (bed 3) is dated to 36,000 ± 2500 ^{14}C yr B.P. (LE-9822). A small willow branch fragment from bed 3 yielded an age of 47,600 +10,200/–4400 ^{14}C yr B.P. (LE-9821). Bed 4, which marks the beginning of the taberite sediments, produced a date of 18,200 +2600/–2200 ^{14}C yr B.P. (LE-9823). This sequence is above bed 1, which holds the mammoth carcass. Considering these dates, the age of the SK mammoth can be estimated at about 40 ka. A direct date on tibia bone, 44,570 +950/–700 ^{14}C yr B.P. (table S2), is consistent with the stratigraphy and the surrounding deposit dates (Fig. 1D). Thus, the SK mammoth carcass is a rare in situ specimen from

[1]Institute for the History of Material Culture, Russian Academy of Sciences, 18 Dvortsovaya Naberezhnaya, St. Petersburg 191186, Russia. [2]Zoological Institute, Russian Academy of Sciences, 1 Universitetskaya Naberezhnaya, St. Petersburg, 199034, Russia. [3]Arctic and Antarctic Research Institute, 38 Bering Street, St. Petersburg, 199397, Russia. [4]Geological Institute, Russian Academy of Sciences, 7 Pyzhevskiy Pereulok, Moscow, 119017, Russia. [5]Budker Institute of Nuclear Physics, Russian Academy of Sciences, Siberian Branch, 11 Academician Lavrentiev Avenue, Novosibirsk, 630090, Russia. [6]St. Petersburg Pediatric Medical University, 2 Litovskaya Street, St. Petersburg, 194100, Russia.
*These authors contributed equally to this work.
†Corresponding author. E-mail: pitulkov@gmail.com

Science

ASASSN-15lh: A highly super-luminous supernova

Subo Dong, B. J. Shappee, J. L. Prieto, S. W. Jha, K. Z. Stanek, T. W.-S. Holoien, C. S. Kochanek, T. A. Thompson, N. Morrell, I. B. Thompson, U. Basu, J. F. Beacom, D. Bersier, J. Brimacombe, J. S. Brown, F. Bufano, Ping Chen, E. Conseil, A. B. Danilet, E. Falco, D. Grupe, S. Kiyota, G. Masi, B. Nicholls, F. Olivares E., G. Pignata, G. Pojmanski, G. V. Simonian, D. M. Szczygiel and P. R. Wozniak

Science **351** (6270), 257-260.
DOI: 10.1126/science.aac9613

The most luminous supernova to date
Supernovae are exploding stars at the end of their lives, providing an input of heavy elements and energy into galaxies. Some types have near-identical peak brightness, but in recent years a new class of superluminous supernovae has been found. Dong *et al.*y report the discovery of ASASSN-15lh (SN 2015L), the most luminous supernova yet found by some margin. It appears to originate in a large quiescent galaxy, in contrast to most super-luminous supernovae, which typically come from star-forming dwarf galaxies. The discovery will provide constraints on models of superluminous supernovae and how they affect their host galaxies.
Science, this issue p. 257